AIP | Applied Physics Letters

Accelerated nanoscale magnetic resonance imaging through phase multiplexing

B. A. Moores, A. Eichler, Y. Tao, H. Takahashi, P. Navaretti, and C. L. Degen

Citation: Applied Physics Letters **106**, 213101 (2015); doi: 10.1063/1.4921409
View online: http://dx.doi.org/10.1063/1.4921409
View Table of Contents: http://scitation.aip.org/content/aip/journal/apl/106/21?ver=pdfcov
Published by the AIP Publishing

Articles you may be interested in

Manipulating spins by cantilever synchronized frequency modulation: A variable resolution magnetic resonance force microscope
Appl. Phys. Lett. **93**, 012506 (2008); 10.1063/1.2955826

Four-channel magnetic resonance imaging receiver using frequency domain multiplexing
Rev. Sci. Instrum. **78**, 015102 (2007); 10.1063/1.2424426

Nanometer-scale magnetic resonance imaging
Rev. Sci. Instrum. **75**, 1175 (2004); 10.1063/1.1666983

Publisher's Note: "Sample-detector coupling in atomic resolution magnetic resonance diffraction" [J. Appl. Phys. 92, 7345 (2002)]
J. Appl. Phys. **93**, 10148 (2003); 10.1063/1.1573218

Sample-detector coupling in atomic resolution magnetic resonance diffraction
J. Appl. Phys. **92**, 7345 (2002); 10.1063/1.1521795

Reuse of AIP Publishing content is subject to the terms at: https://publishing.aip.org/authors/rights-and-permissions. Download to IP: 140.247.233.35 On: Sun, 25 Sep 2016 15:25:54

Accelerated nanoscale magnetic resonance imaging through phase multiplexing

B. A. Moores,[1] A. Eichler,[1,a)] Y. Tao,[1,2] H. Takahashi,[1] P. Navaretti,[1] and C. L. Degen[1]
[1]*Department of Physics, ETH Zurich, Otto-Stern-Weg 1, 8093 Zurich, Switzerland*
[2]*Department of Chemistry, Massachusetts Institute of Technology, 77 Massachusetts Avenue, Cambridge, Massachusetts 02139, USA*

(Received 13 February 2015; accepted 12 April 2015; published online 26 May 2015)

We report a method for accelerated nanoscale nuclear magnetic resonance imaging by detecting several signals in parallel. Our technique relies on phase multiplexing, where the signals from different nuclear spin ensembles are encoded in the phase of an ultrasensitive magnetic detector. We demonstrate this technique by simultaneously acquiring statistically polarized spin signals from two different nuclear species (^{1}H, ^{19}F) and from up to six spatial locations in a nanowire test sample using a magnetic resonance force microscope. We obtain one-dimensional imaging resolution better than 5 nm, and subnanometer positional accuracy. © *2015 AIP Publishing LLC*.
[http://dx.doi.org/10.1063/1.4921409]

Nanoscale magnetic resonance imaging (nanoMRI) is a promising, yet challenging microscopy technique for three-dimensional imaging of single objects with nanometer spatial resolution.[1,2] Among the advantages of nanoMRI are the possibility of site-specific image contrast, the absence of radiation damage, and the fact that only a single copy of an object is required. These qualities are particularly well-suited to provide structural information of large biomolecular complexes that are known to overwhelm nuclear magnetic resonance (NMR) spectroscopy and that evade crystallization for X-ray analysis. Recent proof-of-concept experiments showed that nanoMRI is capable of imaging individual virus particles in three dimensions with <10 nm spatial resolution,[3] as well as isotope-specific image contrast.[4] The best detection sensitivities achieved to date are in the range of $10^1 - 10^4$ statistically polarized nuclear spins.[5–8] NanoMRI has been demonstrated using several ultrasensitive signal detection techniques, especially magnetic resonance force microscopy (MRFM)[9,10] and diamond-based magnetometry.[5,6,11]

Although $\sim$10 nm spatial resolution has been reached in several experiments,[3,4,12] realizing this resolution in three-dimensional images required long averaging times. For instance, imaging the proton density (^{1}H) in a single tobacco mosaic virus required two weeks of data acquisition,[3] even for coarsely sampled data. The long averaging times are prohibitive if one intends to refine voxel sizes or to image multiple nuclear spin species (e.g., ^{1}H and ^{13}C). The slow data acquisition is in part due to the point-by-point measurement procedure where only a small subset of nuclei in a sample is detected at a given time.

An interesting avenue for speeding up the image acquisition process is to measure multiple signals in parallel and to use post processing to calculate the contributions from each individual signal. Signal encoding is especially well-suited for MRI since nuclear spins can be separately addressed by radio-frequency (RF) pulses based on their differing Larmor frequencies. In micron-to-millimeter scale MRI, Fourier-transform[13] and Hadamard[14,15] encoding provide efficient means for detecting the thermal (Boltzmann) polarization of nuclear spins.

When imaging voxels are less than $\sim(100\,\text{nm})^3$, the thermal polarization becomes exceedingly small and is dominated by statistical polarization fluctuations.[16] It is the variance of these statistical fluctuations that then serves as the imaging signal.[17] Since variance measurements cannot be coherently averaged, traditional encoding techniques fail and parallel signal detection is considerably more challenging. One effort for parallel detection of statistical spin polarization included the use of multiple detector frequencies.[18] Unfortunately, this approach is limited by detector bandwidth, and often only a single short-lived spin signal (which is the case for most biological samples) can be accommodated. An exciting prospect is to Fourier encode statistically polarized nuclei by a correlation measurement;[12,19] however, these methods require pulsed gradients or mechanical shuttling and have yet to be applied to 3D imaging.

In this work, we introduce a simple multiplexing technique capable of reducing data acquisition times for statistically polarized spins, irrespective of detector bandwidth or availability of pulsed gradients. Our technique relies on phase multiplexing, whereby spin signals are encoded into the in-phase and quadrature channels of a phase-sensitive nuclear spin detector. We demonstrate the technique by simultaneously acquiring spin signals from different nuclear species and from multiple spatial locations in a nanowire test sample using MRFM. Additionally, we show that the imaging resolution can be improved by subdividing voxels at undiminished signal-to-noise ratio (SNR).

In nanoscale MRI, the number of spins in an imaging voxel is measured as the variance σ_M^2 of the fluctuating nuclear magnetization $M(t)$.[17] Phase-sensitive detection can be obtained by periodically reversing the sign of $M(t)$ to create an oscillating magnetic signal and by synchronizing this ac signal with the detector reference clock.[5,17] The signal is usually evaluated at 0° and 90° with a lock-in amplifier. However, when squaring the signal to calculate its variance,

a)eichlera@phys.ethz.ch

 © 2015 AIP Publishing LLC

Reuse of AIP Publishing content is subject to the terms at: https://publishing.aip.org/authors/rights-and-permissions. Download to IP: 140.247.233.35 On: Sun, 25 Sep 2016 15:25:54

the signs of the two lock-in quadratures are lost and the phase cannot be evaluated. We overcome this problem by demodulating the signal at 0°, 45°, 90°, and 135°. This four-channel lock-in technique allows retrieving the signal phase from the variances of the four channels.[20] It thus reconciles nanoMRI with phase-sensitive detection in the regime of small, statistically polarized spin ensembles.

In MRFM, the detector consists of a micromechanical cantilever that is coupled to the nuclear magnetization by the sharp magnetic gradient G of a nanoscale ferromagnetic tip (see Fig. 1(a)). The cantilever then converts the variance of the magnetic force $\sigma_F^2 = G^2 \times \sigma_M^2$ into a measurable oscillating motion.

Phase multiplexing is achieved by exciting several nuclear spin ensembles simultaneously, while introducing a time delay between magnetization reversals. Since signal detection is phase-sensitive, a time delay τ corresponds to a phase shift $\phi = 2\pi\tau/T$, where $T = 1/f_c$ is the duration of one clock cycle and f_c is the detector frequency. When measuring N statistically independent spin ensembles, the total (complex) signal E is

$$E = \sum_{j=1}^{N} S_j e^{i2\phi_j}, \tag{1}$$

where $S_j = \sigma_{M_j}^2$ is the variance of the jth ensemble's magnetization $M_j(t)$ and ϕ_j denotes the phase shift of the periodic reversal of $M_j(t)$ relative to the detector clock.[20] In order to separate the different signal components, one may carry out N measurements, each with a different combination of phases, yielding $\vec{E} = (E_1, E_2, ..., E_N)$. The reconstruction of the original spin signals $\vec{S} = (S_1, S_2, ..., S_N)$ then follows by linear recombination as

$$\vec{S} = \mathbf{A}^{-1}\vec{E}, \tag{2}$$

where the transfer matrix

$$\mathbf{A} = \begin{bmatrix} e^{i2\phi_{11}} & e^{i2\phi_{12}} & \dots & e^{i2\phi_{1N}} \\ e^{i2\phi_{21}} & e^{i2\phi_{22}} & \dots & e^{i2\phi_{2N}} \\ \vdots & \vdots & \ddots & \vdots \\ e^{i2\phi_{N1}} & e^{i2\phi_{N2}} & \dots & e^{i2\phi_{NN}} \end{bmatrix}$$

contains the phase of each spin inversion during the cantilever period, as depicted in Fig. 1(d). The phase at which the spin signal due to the jth ensemble appears changes between different experiments k. Although any linearly independent set of phases ϕ_{jk} will allow for the reconstruction of $\vec{S}$, only a suitable choice of ϕ_{jk} will evade amplification of detector noise.[20]

Since each measurement E_k simultaneously detects the magnetization of all nuclear ensembles, the signal collected after a complete sequence $\vec{E}$ is N times larger compared to a sequential collection of $S_1, ..., S_N$ without multiplexing. By contrast, the same amount of detector noise is added to each measurement E_k regardless of whether multiplexing is applied. Phase multiplexing can therefore improve the SNR by $\sqrt{N}$ for a fixed acquisition time. Alternatively, the acquisition time can be reduced by N without any loss in SNR.

Whether the improvement by N is realized depends on the choice of phases ϕ_{jk}. Poorly selected phases will amplify detector noise when reconstructing $\vec{S}$ from $\vec{E}$. We find that for white detector noise (such as thermal noise), the noise amplification factor is given by the matrix 2-norm: $||\mathbf{A}^{-1}||_2 = (\sum_{jk}|\tilde{a}_{jk}|^2)^{1/2} \geq 1$, where $\tilde{a}_{jk}$ are the matrix elements of $\mathbf{A}^{-1}$.[20] For an optimum set of phases $||\mathbf{A}^{-1}||_2 = 1$. Although such an optimum set can be constructed (e.g., using the digital Fourier transform matrix $\phi_{jk} = \pi jk/N$), we used a heuristic search in order to satisfy additional constraints, especially peak RF pulse power. Other potential

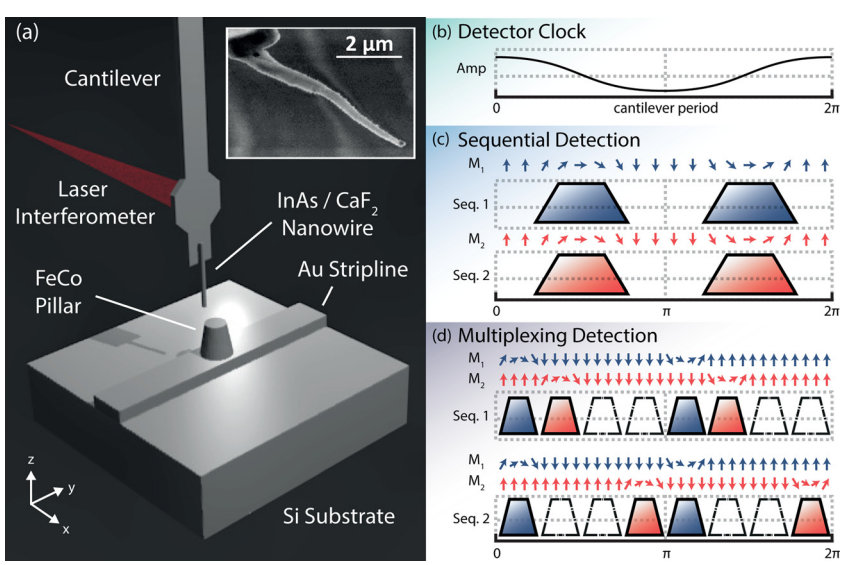

FIG. 1. Basic principle of phase multiplexing with $N = 2$ nuclear spin ensembles. (a) Schematic representation of the MRFM apparatus showing a micromechanical cantilever and ferromagnetic tip. Inset: Scanning electron micrograph of an InAs nanowire test sample attached to the cantilever end. The nanowire is possibly terminated by a Au catalyst particle. (b) Cantilever detector clock. (c) For sequential measurements, only a single nuclear spin ensemble is flipped at a time. Arrows depict the orientation of nuclear magnetization $M_j(t)$ and trapezoids symbolize adiabatic RF pulses.[20] (d) For phase multiplexed measurements, both nuclear spin ensembles are flipped, but the flipping is partially out of phase. Two different flipping sequences are applied to generate two different measurements E_1 and E_2, which are subsequently reconstructed to yield S_1 and S_2. Encoding phases in this example are $\phi_{11} = 22.5°$, $\phi_{12} = 67.5°$ (for E_1) and $\phi_{21} = 22.5°$, $\phi_{22} = 157.5°$ (for E_2).

Reuse of AIP Publishing content is subject to the terms at: https://publishing.aip.org/authors/rights-and-permissions. Download to IP: 140.247.233.35 On: Sun, 25 Sep 2016 15:25:54

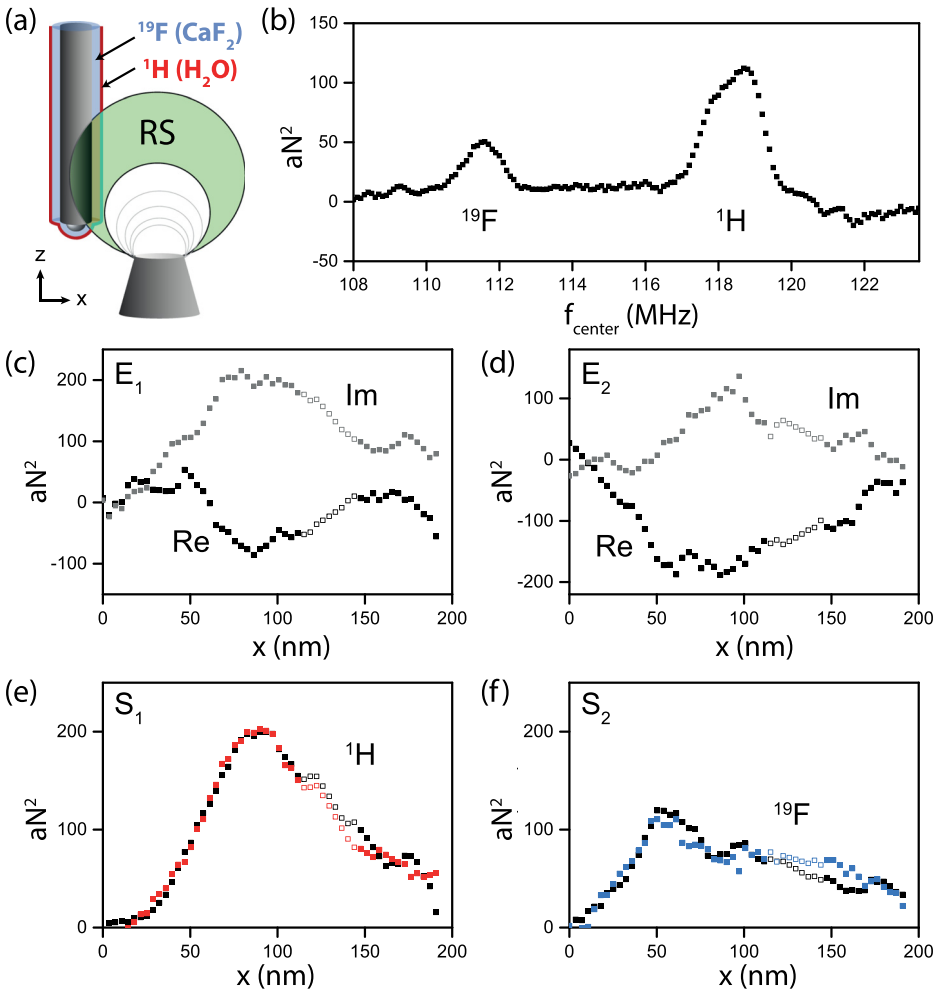

FIG. 2. (a) Schematic of the nanowire with ^{19}F and ^{1}H layers. RS represents the resonant slice, i.e., the volume in space where nuclear spins contribute to the signal. (b) NMR spectrum of the sample measured by incrementing the RF center frequency f_{center}, while the nanowire was at a fixed position. In a magnetic field of 2.77 T, the Larmor frequency of ^{1}H is 118.0 MHz and of ^{19}F is 110.9 MHz. Each data point was averaged for 360 s. (c) and (d) One-dimensional x scans (3.6 nm steps) at a fixed height using the multiplexing sequences of Fig. 1(d). Black and gray symbols represent the real and imaginary parts of E_1 and E_2, respectively. RF center frequencies were 118.0 MHz and 110.9 MHz with $\Delta f_{\text{dev}} = 0.5$ MHz. (e) and (f) Reconstructed signal (colored squares) providing separate images for (e) ^{1}H and (f) ^{19}F. A sequential single isotope scan is shown for comparison (black squares). Total averaging time per point was 240 s for multiplexed acquisition and 480 s for sequential acquisition. For reasons explained in Ref. 20, the mechanical detector was unstable between 115 nm and 145 nm. Data in this range was replaced by interpolated data, represented by hollow symbols in (c)–(f). Data have been spatially low pass filtered by 5 points.

noise sources include spin noise,[17] correlations between spin ensembles, and instabilities in detector phase, gain, or frequency.[20]

We demonstrated phase multiplexing by measuring the statistical polarization of $\sim 10^5$ ^{1}H and ^{19}F spins on an InAs nanowire test sample. The nanowire had a diameter of 120 nm and was coated with 60 nm of CaF_2 by thermal evaporation (see Fig. 2(a)). ^{1}H spins were present in a $\sim$1 nm layer of surface adsorbates that naturally formed in ambient air.[3,4,7] For nanoscale MRI measurements, the nanowire was attached to the end of an ultrasensitive silicon cantilever and mounted in an MRFM apparatus operating at 4.2 K temperature and 2.77 T magnetic bias field. Under measurement conditions, the cantilever had a resonant frequency $f_c \sim 5$ kHz, a spring constant $k_c \sim 2.5 \times 10^{-4}$ N/m, and a mechanical $Q \sim 30,000$, equivalent to a thermal force noise of about $3\,\text{aN}/\sqrt{\text{Hz}}$. For the imaging, the nanowire was approached to within 100 nm of a 300-nm-diameter FeCo magnetic tip.[21]

Nuclear magnetization reversals were performed using periodic application of adiabatic RF pulses. These pulses had a center frequency f_{center} and bandwidth of $2\Delta f_{\text{dev}}$. They inverted nuclear spins only in a thin "resonance slice" (RS) in space whose Larmor frequencies $f_L = \gamma_n B$ lay within $f_{\text{center}} \pm \Delta f_{\text{dev}}$, where B is the magnetic field at a spin's location (see Fig. 2(a)) and γ_n is the nuclear gyromagnetic ratio. For the multiplexing, several adiabatic pulses with different center frequencies f_{center} were co-added.[21] Signal detection used a fiber-optic interferometer to read out the cantilever oscillation, and four-phase lock-in demodulation to extract the complex signal variance E.[20]

In a first experiment, we performed multiplexing of two different nuclear isotopes (^{1}H and ^{19}F). In order to identify the nuclear species, we parked the nanowire $\sim$60 nm above the nanomagnetic tip and measured the nuclear magnetization as a function of RF center frequency (Fig. 2(b)). Two peaks at 111 MHz and 118 MHz confirmed the presence of both ^{1}H and ^{19}F nuclear species. To demonstrate multiplexing, we performed a one-dimensional spatial scan over the magnetic tip while exciting both ^{1}H and ^{19}F. At each location, $N = 2$ signals were acquired with different phase sequences, resulting in the two scans E_1 and E_2 shown in Figs. 2(c) and 2(d). Application of Eq. (2) then directly reproduced the reconstructed signals (Figs. 2(e) and 2(f)). We found excellent agreement between reconstructed signals and sequential control measurements of ^{1}H and ^{19}F.

In addition to chemical contrast imaging, multiplexing can also be applied to detect signals of the same isotope in different spatial regions of a sample. Such multi-slice imaging provides depth information with a single lateral scan, and may be useful to improve the fidelity of 3D image reconstruction. Fig. 3(a) shows an example of spatial multiplexing by detecting $N = 6$ resonant slices of ^{1}H. A shifting peak is seen as the

Reuse of AIP Publishing content is subject to the terms at: https://publishing.aip.org/authors/rights-and-permissions. Download to IP: 140.247.233.35 On: Sun, 25 Sep 2016 15:25:54

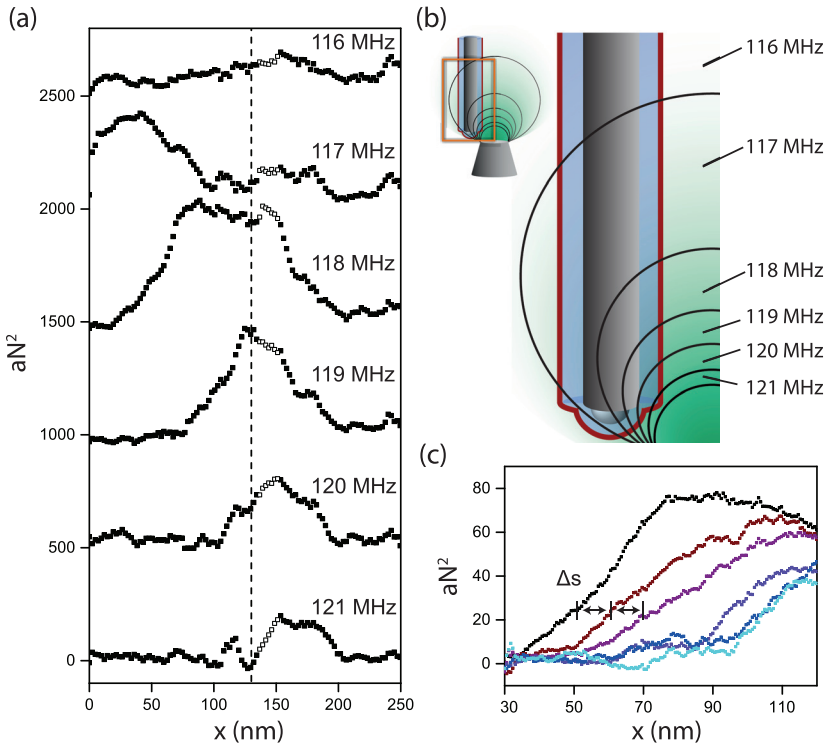

FIG. 3. (a) Signal from $N = 6$ different ^{1}H ensembles measured during a single x scan with phase multiplexing. x increment was 2.4 nm, $\Delta f_{dev} = 0.3$ MHz, and center frequencies of resonant slices ranged from 116 to 121 MHz as indicated. The averaging time was 360 s at each position for all 6 measurements together. As in Fig. 2, hollow points represent data that were interpolated due to instability of the mechanical oscillator.[20] Data were low pass filtered by 5 points. (b) Schematic of the spatial shape of resonant slices associated with Larmor frequencies 116 – 121 MHz. As the nanowire is scanned from left to right, spins intersect slices with progressively higher Larmor frequencies, reflected in a shifting peak in (a). The schematic corresponds to the x location of the vertical dotted line. (c) High resolution x scan with increments of 0.6 nm, $\Delta f_{dev} = 0.13$ MHz, and slice center frequencies ranging from 117.8 to 119.8 MHz in steps of 0.4 MHz (from left to right). Averaging time was 1080 s at each position for all 6 measurements together. Data were low pass filtered by 30 points.

nanowire moves across the different slices, and the six signal traces clearly reflect the geometry of imaging slice and nanowire.

We have tested multiplexing down to very low values of Δf_{dev} to estimate the limits towards high spatial resolution. Figure 3(c) shows such a high resolution scan acquired with frequency increments of $\Delta f_{center} = 0.4$ MHz. By comparing the signal onset as a function of x position, we find that the lateral distance between slices Δs is about 10 nm. This corresponds to a lateral magnetic gradient of $G = \partial B_z/\partial x = \Delta f_{center}/(\gamma_n \Delta s) \approx 1 \times 10^6$ T/m. A comparison with similar nanomagnetic tips, where $G \sim 4 - 5 \times 10^6$ T/m,[22] indicates that our tip had a lower-than-expected gradient, probably due to partial oxidation. Note that the imaging resolution is not limited by the step size Δs, but by the bandwidth of the frequency modulation $\Delta f_{dev} = 0.13$ MHz. As the full width at half maximum of the resonant slice is approximately $\sqrt{2}\Delta f_{dev}$,[3] the imaging resolution is about $\sqrt{2}\Delta f_{dev}/(\gamma_n G) \approx 4.3$ nm. With an improved nanomagnetic tip, an imaging resolution of ~1 nm can therefore be expected.

To compare the quality of multiplexed data to that of sequential measurements, we have quantified the signal error by analyzing the standard deviation of point-to-point fluctuations in the datasets. For the multiplexed scans in Figs. 2(e) and 2(f), we find $\epsilon_H = 6.62$ aN^2 and $\epsilon_F = 6.53$ aN^2, while the separate measurements have $\epsilon_H = 6.89$ aN^2 and $\epsilon_F = 4.94$ aN^2. The differences in amplitude between multiplexed and separately measured signals have standard deviations of 6.31 aN^2 for ^{1}H and 8.34 aN^2 for ^{19}F.[20] These results confirm that phase multiplexing produces the same signal amplitude and SNR as sequential acquisition within half the averaging time.

While imaging step sizes and resolution for our experiments were on the order of a few nanometers, we found that the imaging precision was below 1 nm. For example, in the leftmost trace of Fig. 3(c) (117.8 MHz center frequency), we observed that the signal rose with 3.4 aN^2/nm around $x \sim 65$ nm. Comparing this slope with the measurement error $\epsilon_H = 0.8$ aN^2, we derive a position uncertainty of 0.24 nm. Although this precision is probably overestimated, we note that the signal onsets of the two scans in Fig. 2(e) coincide within 0.6 nm.[20] Such good positional accuracy is an important prerequisite for extending nanoMRI to subnanometer resolution.

Finally, we briefly comment on the limits of phase-multiplexed detection. When applying N RF frequencies simultaneously, both average and peak power increase by at least N regardless of the finer details of RF pulses. Phase multiplexing therefore puts progressive demands on RF excitation, which in our experiments limited $N < 10$. Moreover, error analysis shows that strong signals tend to transmit noise to weak signals and eventually deteriorate the SNR of the latter,[20] which we found to become noticeable as $N > 6$.

In summary, we have introduced a simple phase multiplexing method for accelerated detection of nanoscale NMR signals. The method is applicable even if spin ensembles are randomly polarized. It can, in principle, be used with any phase-sensitive excitation/detection scheme, including those used in recent diamond-based magnetometry experiments.[5,23]

Reuse of AIP Publishing content is subject to the terms at: https://publishing.aip.org/authors/rights-and-permissions. Download to IP: 140.247.233.35 On: Sun, 25 Sep 2016 15:25:54

Using an MRFM apparatus, we have demonstrated simultaneous acquisition of nuclear spin signals from two different nuclear species and from up to six different sections within a sample. One-dimensional imaging scans reached a nominal spatial resolution <5 nm with subnanometer positional accuracy. The reduction in measurement time offered by our technique will be especially useful for 3D images of biomolecular complexes with isotope contrast.

We thank Cecil Barengo, Urs Grob, Christoph Keck, Heike Riel, and the Physics machine shop for providing samples and experimental assistance. We also appreciate the insightful discussions with Martino Poggio, Fei Xue, and Benedikt Herzog. This work has been supported by the ERC through Starting Grant 309301, and by the Swiss NSF through the NCCR QSIT. B.A.M. acknowledges an NSERC fellowship.

[1]J. A. Sidles, Appl. Phys. Lett. **58**, 2854 (1991).
[2]C. L. Degen, Appl. Phys. Lett. **92**, 243111 (2008).
[3]C. L. Degen, M. Poggio, H. J. Mamin, C. T. Rettner, and D. Rugar, Proc. Natl. Acad. Sci. U.S.A. **106**, 1313 (2009).
[4]H. J. Mamin, T. H. Oosterkamp, M. Poggio, C. L. Degen, C. T. Rettner, and D. Rugar, Nano. Lett. **9**, 3020 (2009).
[5]H. J. Mamin, M. Kim, M. H. Sherwood, C. T. Rettner, K. Ohno, D. D. Awschalom, and D. Rugar, Science **339**, 557 (2013).
[6]T. Staudacher, F. Shi, S. Pezzagna, J. Meijer, J. Du, C. A. Meriles, F. Reinhard, and J. Wrachtrup, Science **339**, 561 (2013).
[7]M. Loretz, S. Pezzagna, J. Meijer, and C. L. Degen, Appl. Phys. Lett. **104**, 33102 (2014).
[8]C. Muller, X. Kong, J. M. Cai, K. Melentijevic, A. Stacey, M. Markham, D. Twitchen, J. Isoya, S. Pezzagna, J. Meijer, J. F. Du, M. B. Plenio, B. Naydenov, L. P. McGuinness, and F. Jelezko, Nat. Commun. **5**, 4703 (2014).
[9]J. A. Sidles, J. L. Garbini, K. J. Bruland, D. Rugar, O. Züger, S. Hoen, and C. S. Yannoni, Rev. Mod. Phys. **67**, 249 (1995).
[10]M. Poggio and C. L. Degen, Nanotechnology **21**, 342001 (2010).
[11]R. Schirhagl, K. Chang, M. Loretz, and C. L. Degen, Annu. Rev. Phys. Chem. **65**, 83 (2014).
[12]J. M. Nichol, T. R. Naibert, E. R. Hemesath, L. J. Lauhon, and R. Budakian, Phys. Rev. X **3**, 031016 (2013).
[13]A. Kumar, D. Welti, and R. R. Ernst, J. Magn. Reson. **18**, 69 (1975).
[14]L. Bolinger and J. S. Leigh, J. Magn. Reson. **80**, 162 (1988).
[15]K. W. Eberhardt, C. L. Degen, and B. H. Meier, Phys. Rev. B **76**, 180405 (2007).
[16]B. E. Herzog, D. Cadeddu, F. Xue, P. Peddibhotla, and M. Poggio, Appl. Phys. Lett. **105**, 043112 (2014).
[17]C. L. Degen, M. Poggio, H. J. Mamin, and D. Rugar, Phys. Rev. Lett. **99**, 250601 (2007).
[18]T. H. Oosterkamp, M. Poggio, C. L. Degen, H. J. Mamin, and D. Rugar, Appl. Phys. Lett. **96**, 083107 (2010).
[19]J. Kempf and J. A. Marohn, Phys. Rev. Lett. **90**, 087601 (2003).
[20]See supplementary material at http://dx.doi.org/10.1063/1.4921409 for details concerning the measurement technique, error propagation, and noise analysis.
[21]M. Poggio, C. L. Degen, C. T. Rettner, H. J. Mamin, and D. Rugar, Appl. Phys. Lett. **90**, 263111 (2007).
[22]H. J. Mamin, C. T. Rettner, M. H. Sherwood, L. Gao, and D. Rugar, Appl. Phys. Lett. **100**, 013102 (2012).
[23]S. Kotler, N. Akerman, Y. Glickman, A. Keselman, and R. Ozeri, Nature **473**, 61 (2011).

Reuse of AIP Publishing content is subject to the terms at: https://publishing.aip.org/authors/rights-and-permissions. Download to IP: 140.247.233.35 On: Sun, 25 Sep 2016 15:25:54